JOMDI

Journal of Medical and Dental Investigations

J Med Dent Invest 2024; 5: e240387
https://doi.org/10.5577/jomdi.e240387

Original Article Open Access

Topographic and morphometric feature of the anatomical structures located in the parapetrosal triangle borderlines

Nilgün Tuncel Çini[1], Semahat Doğru Yuvarlakbaş[2], Serdar Babacan[3]

[1] Bilecik Şeyh Edebali University, Faculty of Medicine, Department of Anatomy, Bilecik, Türkiye
[2] Harran University, Faculty of Medicine, Department of Anatomy, Şanlıurfa, Türkiye
[3] Bursa Uludağ University, Faculty of Medicine, Department of Anatomy, Bursa, Türkiye

Abstract

Aim: The parapetrosal triangle, which is one of the landmarks and regions determined to provide orientation to the skull base, has the importance that it can guide the topographic anatomy of the paraclival region from an exocranial perspective. The study aimed to determine the topographic anatomy of the parapetrosal region and the relationships between the distances between the foramina within the triangle.

Methods: The study was carried out on a total of 17 bones belonging to 34 sides. Eighteen parameters were determined to be examined on digital images, and all measurements were carried out by the same researcher on both sides. We compared the morphometric features of the right and left sides via the Student's T-test and Mann-Whitney U test. We evaluated the relationship between variables through Pearson and Spearman correlation analyses. We developed equations to estimate the morphometric features located in the parapetrosal triangle using the bispinal line.

Results: It was observed that there was no difference between the sides for any variable. We found the distance between the HS and midline 5.37±0.68 cm for the right side and 5.39±0.60 cm for the left side. We found the bispinal distance value obtained by adding the right and left midline distances, and this was determined to be 10.76±1.22 cm on average. We found the spinopterygoidal line distance 6.70±0.81 cm and 6.75±0.86 cm for the right and left sides, respectively. We developed equations to estimate the location of some anatomical structures using Henle's spine. The equation was: the distance between the HS and midline = 0.005 + (0.005 x length of the bispinal line); Adjusted R^2 value was 0.899.

Conclusion: As a result of the high-reliability models that we created by taking the parapetrosal triangle as a reference, we showed that Henle's spine is a reliable reference point by the literature with a different method. We believe that the study will be an important guide for surgeons.

Keywords: Parapetrosal triangle, Henle's spine, foramen ovale, carotid canal, regression

Received: 7 November 2024
Accepted: 26 December 2024
Published: 31 December 2024

Correspondence:

Dr. Nilgün TUNCEL ÇİNİ
Bilecik Şeyh Edebali University, Faculty of Medicine, Department of Anatomy, Bilecik, Türkiye
E-mail: nilgun.cini@bilecik.edu.tr

How to cite this article:

Tuncel Çini N, Doğru Yuvarlakbaş S, Babacan S. Topographic and morphometric feature of the anatomical structures located in the parapetrosal triangle borderlines. J Med Dent Invest 2024;5:e240387. https://doi.org/10.5577/jomdi.e240387

Introduction

The base of the skull, which forms the base of the cranial cavity, both connects the anatomical structures in the neck to the cranial cavity and surrounds the brain, separating it from other anatomical structures (1-3). The base of the skull is a very complex structure with many foramina where nerves and vessels enter and exit, muscle attachment surfaces, and bony protrusions (1, 2). Due to the presence of these complex structures, the base of the skull is a difficult region for neurosurgeons and oncosurgeons. The surgical approaches to this region have not yet been standardized (3-6). Neurosurgeons have attempted to compensate for this complexity by establishing various relationships between the anatomical structures at the skull base in order to orient the skull base to guide surgical dissections (7).

The parapetrosal triangle, which is one of the landmarks and regions determined to provide orientation to the skull base, was first described in 2005 by Ulug et al. The importance of this area is that it can guide the topographic anatomy of the paraclival region from an exocranial perspective (3, 7). The parapetrosal triangle is also one of the useful guides during the infratemporal fossa approach, the middle cranial fossa internal and posterior approaches (8-10). Briefly, this triangle is the region between the spinopterygoidal line (spine of Henle to foramen ovale) bispinal line (between 2 spines of Henle), and midsagittal line (posterior margin of the medial pterygoid plate) on both the right and left sides (6, 7). The vertices of this triangle are formed by the intersection of the spinopterygoidal, bispinal, and midsagittal lines. These lines can be described as follows: the bispinal line lies between the two spines of Henle, the spinopterygoidal line extends from the spine of Henle at the posterior margin of the medial pterygoid plate to the medial margin of the foramen ovale, and the midsagittal line originates at the posterior margin of the medial pterygoid plate and is essentially the right bisector of the bispinal line (6, 9).

The parapetrosal triangle encompasses almost all the major structures of the skull base (10). Within the boundaries of the parapetrosal triangle are very important skull base foramina and the anatomical structures that pass through these foramina. The main important anatomical structures within the boundaries of the triangle are the sphenoid spine, foramen spinosum, foramen ovale, root of lateral and medial pterygoid plate, vomer, stylomastoid foramen, jugular foramen, occipital condyle, external orifice of hypoglossal canal, foramen magnum, petrosal internal carotid artery, jugular bulb, petrosal nerves, foramen spinosum (6, 9).

The aim of the study was to determine the topographic anatomy of the parapetrosal region and to determine the correlation between the distances between the foramina within the triangle.

Materials and Methods

The study was carried out on a total of 17 bones belonging to 34 sides in the Anatomy Departments of Bilecik Seyh Edebali University and Harran University Medical Faculties. Bones with deformities or fractures in the measured area were excluded from this study. The age and gender of the bones are unknown. The photographs were taken in a stable position, using the ruler on the sides for the calibration. The photos were measured in centimeters after their calibrations. The measurements were performed by the same researcher. Eighteen parameters were determined to be examined on digital images, and all measurements were carried out by the same researcher on both sides (Fig. 1).

While determining the measurement parameters, Henle's spine (HS), bispinal line, and spinopterygoidal line, which are the reference points of the parapetrosal triangle, were used (6,9).

The following measurements are (9):

1. The distance between the HS and midline
2. The distance between the HS and midline on the spinopterygoid line (line passing through the oval foramen from HS to the midline)
3. The distance between the points where the midline intersects the spinopterygoid line and the spinal line
4. The distance between the HS and the lateral tip of the foramen jugulare
5. The distance between the HS and the medial tip of the foramen jugulare
6. The distance between the HS and the lateral tip of the canalis caroticus
7. The distance between the HS and the medial tip of the canalis caroticus
8. The distance between the HS and the anterior tip of the foramen lacerum
9. The distance between the HS and the posterior tip of the foramen lacerum
10. The minimum length of the foramen jugulare
11. The maximum length of the foramen jugulare
12. The minimum length of the canalis caroticus
13. The maximum length of the canalis caroticus
14. The minimum length of the foramen lacerum
15. The maximum length of the foramen lacerum
16. The angle between the bispinal line and spinopterygoidal line
17. The angle between the bispinal line and midline
18. The angle between the midline and spinopterygoidal line

Statistical analysis

Analyses were performed by using IBM SPSS 26.0 software (IBM Inc., Armonk, NY, USA).

Normality values of the parameters were evaluated with the Kolmogorov-Smirnov test. Student's T-test and Mann-Whitney U test were used for right and left-side comparisons. It was aimed to determine the relationship between variables through Pearson and Spearman correlation analyses (p<0.05).

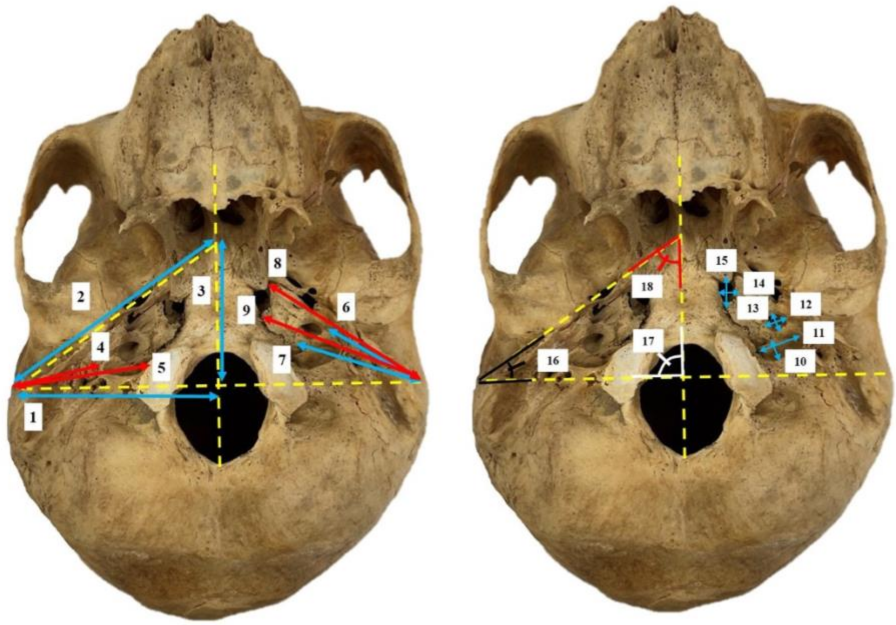

Figure 1. The dashed yellow lines show the parapetrosal triangle, and the measured parameters are included in the figure.

Results

Descriptive statistics for each parameter are given as mean± standard deviation in centimeters for both sides (Table 1). It was observed that there was no difference between the sides for any variable. The distance between the HS and midline was 5.37±0.68 cm for the right side and 5.39±0.60 cm for the left side. The bispinal distance value was obtained by adding the right and left midline distances, and this was determined to be 10.76±1.22 cm on average. The spinopterygoidal line distance was also 6.70±0.81 cm and 6.75±0.86 cm for the right and left sides, respectively. The distance between the points where the midline intersects the spinopterygoid line and the spinal line has been determined as 3.94±0.74 cm for the right and 4.01±0.82 cm for the left side. The internal angle values of the parapetrosal triangle that emerges when these edges are joined have been evaluated in the study. Accordingly, the angle between the bispinal line and spinopterygoidal line were 36.36°±5.07° and 35.73°±5.22°; the angle between the bispinal line and midline were 89.63°±2.30° and 84.10°-93.65°; the angle between the midline and spinopterygoidal line were 53.75°±5.03° and 45.91°-66.16° for the right and left side respectively. The distances of the HS to the edges of the foramen lacerum, canalis caroticus, and foramen jugulare and the morphometric data of the foramens and canal were also given in Table 1.

As a result of correlation analysis, it was observed that there were high correlation coefficient values between some parameters. It was determined that these values were largely similar for the right and left sides. Among these coefficient values, results with values of 0.70 and above were evaluated in the study. It was observed that bispinal distance was especially highly correlated with some parameters. The distance between the HS - midline was correlated with the bispinal line, and the r value was 0.944 for the right and 0.945 for the left side. The distance between the HS and midline on the spinopterygoid line was also correlated with the bispinal line, and the r value was 0.737 and 0.827 for the right and left sides, respectively. High correlation coefficients were found between the distance of the HS to the median error and the spinopterygoidal line length (r=0.806 for the right and r=0.836 for the left). It was observed that there was a relationship between the distance of the HS to the median line and the distance of the HS to the foramen lacerum. The r value for the distance from the anterior margin of the foramen lacerum was 0.814 on the right and 0.863 on the left, while the correlation coefficient for the distance from the posterior margin of the foramen was 0.890 for the right and 0.907 for the left. Similar correlations were detected for the foramen lacerum, the distance between the HS and midline on the spinopterygoid line, and the distance between the points where the midline intersects the spinopterygoid line and the spinal line

Table 1. Descriptive statistics of the parameters as given mean±standart deviation (cm)

	Right		Left		
Parameter	Mean±SD	Range	Mean±SD	Range	*p*-value
1	5.37±0.68	4.11-6.35	5.39±0.60	4.45-6.40	0.951
2	6.70±0.81	5.22-8.19	6.75±0.86	5.41-8.15	0.858
3	3.94±0.74	2.53-5.53	4.01±0.82	2.88-5.61	0.792
4	1.68±0.29	1.24-2.26	1.78±0.39	1.25-2.41	0.395
5	3.15±0.41	2.46-3.95	3.15±0.37	2.53-3.91	0.997
6	2.23±0.36	1.59-2.85	2.33±0.40	1.56-3.05	0.469
7	3.01±0.38	2.35-3.74	3.10±0.47	2.14-4.00	0.542
8	4.70±0.65	3.77-5.85	4.77±0.70	3.61-5.79	0.767
9	4.23±0.71	3.18-6.05	4.25±0.55	3.45-5.15	0.936
10	0.68±0.21	0.28-1.14	0.58±0.19	0.27-0.95	0.144
11	1.48±0.25	0.92-1.83	1.37±0.32	0.94-1.91	0.299
12*	0.53±0.06	0.36-0.60	0.53±0.09	0.42-0.74	0.946
13	0.80±0.09	0.65-0.91	0.75±0.13	0.53-1.09	0.168
14	0.54±0.17	0.31-0.85	0.56±0.17	0.33-0.89	0.744
15	1.22±0.22	0.80-1.63	1.20±0.28	0.75-1.64	0.855
16	36.36°±5.07°	24.20°-43.30°	35.73°±5.22°	24.77°-47.06°	0.724
17	89.63°±2.30°	85.30°-95.13°	90.14°±2.61°	84.10°-93.65°	0.549
18	53.75°±5.03°	46.58°-66.96°	54.48°±5.55°	45.91°-66.16°	0.690

*Non-parametric variable

For angular measurements, the angle between the bispinal line and spinopterygoidal line and the angle between the midline and spinopterygoidal line were also correlated (r=-0.944 for the right and r=-0.830 for the left side). The parameters and correlation coefficient values related to each other are given in Table 2. It was determined that there was no correlation between the angular values and linear parameters. Since statistically low coefficient correlation values would have low regression values, these values were not evaluated in the study. Regression analysis was performed to estimate the relevant anatomical structures using parameters with high correlation between them, and some formulas were produced. The formulas produced are shown in Table 3. The best formula was for the distance between the HS and midline; the formula was 0.005 + (0.005 x length of the bispinal line). The adjusted R^2 value was 0.899, and the standard error was 0.20.

A graphical illustration of the study is shown in Figure 2.

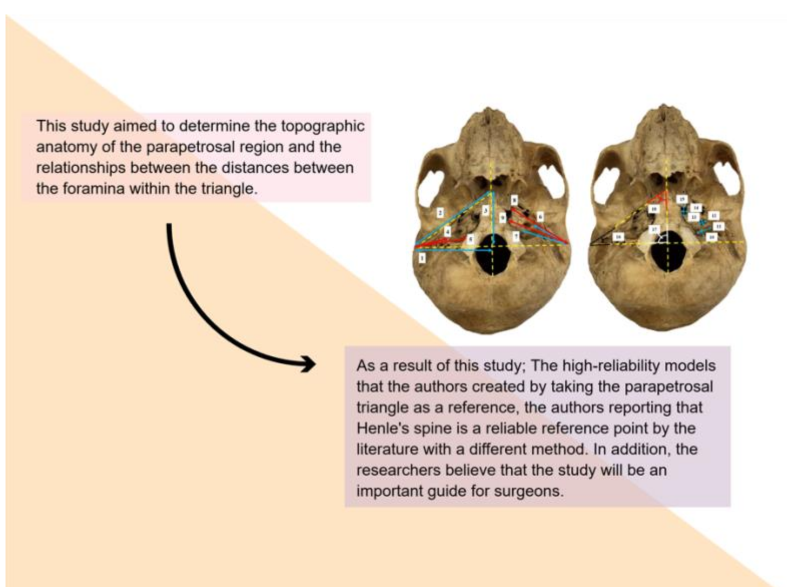

Figure 2. Graphical illustration of the study

Table 2. Correlations between the parameters and r values

	r value	
Correlated Parameters	Right	Left
The distance between the HS and midline - the distance between the HS and midline on the spinopterygoid line	0.806	0.836
The distance between the HS and midline - the distance between the HS and the medial tip of the foramen jugulare	0.718	0.747
The distance between the HS and midline - the distance between the HS and the anterior tip of the foramen lacerum	0.814	0.863
The distance between the HS and midline - the distance between the HS and the posterior tip of the foramen lacerum	0.890	0.907
The distance between the HS and midline on the spinopterygoid line - the distance between the points where the midline intersects the spinopterygoid line and the spinal line	0.738	0.829
The distance between the HS and midline on the spinopterygoid line - the distance between the HS and the anterior tip of the foramen lacerum	0.873	0.760
The distance between the HS and midline on the spinopterygoid line - the distance between the HS and the posterior tip of the foramen lacerum	0.863	0.708
The distance between the HS and the lateral tip of the foramen jugulare - the distance between the HS and the lateral tip of the canalis caroticus	0.826	0.809
The distance between the HS and the lateral tip of the foramen jugulare - the distance between the HS and the medial tip of the canalis caroticus	0.786	0.823
The distance between the HS and the medial tip of the foramen jugulare - the distance between the HS and the lateral tip of the canalis caroticus	0.870	0.777
The distance between the HS and the medial tip of the foramen jugulare - the distance between the HS and the medial tip of the canalis caroticus	0.869	0.786
The distance between the HS and the medial tip of the foramen jugulare - the distance between the HS and the posterior tip of the foramen lacerum	0.738	0.862
The distance between the HS and the lateral tip of the canalis caroticus - the distance between the HS and the medial tip of the canalis caroticus	0.952	0.972
The distance between the HS and the lateral tip of the canalis caroticus - the distance between the HS and the anterior tip of the foramen lacerum	0.802	0.762
The distance between the HS and the lateral tip of the canalis caroticus - the distance between the HS and the posterior tip of the foramen lacerum	0.725	0.826
The distance between the HS and the medial tip of the canalis caroticus - the distance between the HS and the anterior tip of the foramen lacerum	0.833	0.829
The distance between the HS and the medial tip of the canalis caroticus - the distance between the HS and the posterior tip of the foramen lacerum	0.728	0.838
The distance between the HS and the anterior tip of the foramen lacerum - the distance between the HS and the posterior tip of the foramen lacerum	0.904	0.818
The distance between the HS and midline - the distance between the bispinal line	0.944	0.945
The distance between the HS and midline - the distance between the HS and midline on the spinopterygoid line	0.737	0.827
The distance between the HS and midline - the distance between the HS and the medial tip of the foramen jugulare	0.720	0.766
The distance between the HS and midline - the distance between the HS and the posterior tip of the foramen lacerum	0.880	0.855
The angle between the bispinal line and spinopterygoidal line - the angle between the midline and spinopterygoidal line	-0.944	-0.830

Table 3. Linear regression equations estimating the morphometric features of anatomical structures at the skull base with reference to the length of the bispinal line

Equation	Adjusted R^2	Standard error of the estimate
The distance between the HS and midline = **0.005 + (0.005 x length of the bispinal line)**	0.899	0.20
The distance between the HS and midline on the spinopterygoid line = **0.659 + (0.564 x length of the bispinal line)**	0.661	0.48
The distance between the HS and the medial tip of the foramen jugulare = **0.546 + (0.0.242 x length of the bispinal line)**	0.557	0.26
The distance between the HS and the lateral tip of the canalis caroticus = **0.227 + (0.191 x length of the bispinal line)**	0.345	0.30
The distance between the HS and the medial tip of the canalis caroticus = **0.469 + (0.240 x length of the bispinal line)**	0.444	0.32
The distance between the HS and the anterior tip of the foramen lacerum = **-0,374+ (0.475 x length of the bispinal line)**	0.717	0.35
The distance between the HS and the posterior tip of the foramen lacerum = **-0.395 + (0.431 x length of the bispinal line)**	0.678	0.36

Discussion

Henle's spine is frequently used by surgeons because it can be easily localized and is a reliable point in interventions on the skull base. It is also of particular importance because it forms the outer border of the parapetrosal triangle, which contains important skull base formations such as the internal carotid artery, jugular bulb, some important cranial nerves, and the intracranial passage of the middle meningeal artery. In addition to the already limited literature information, we tried to localize this point clearly in the existing study, and with the high-rate regression formulas we obtained, we showed that this point is reliable with mathematical models. Determining the precise intervention areas and distances specific to the person rather than guessing will guide surgeons in the interventions to be made in the region through the formulas obtained. With this study, we have also shown that Henle's spine, which is used as a reference in many surgical procedures and is stated as reliable in the literature (11,12), is a suitable point within the parapetrosal triangle and its structure.

When we compared the obtained data with the literature, we saw that some parameters had lower values than existing studies. The linear distance values between HS and the lateral margin of the carotid canal were determined as 2.23±0.36 cm for the right and 2.33±0.40 cm for the left. The linear distance values between HS and the medial margin of the carotid canal were also determined as 3.01±0.38 cm for the right and 3.10±0.47 cm for the left in our study. Ulug et al. reported 28.7±3.7 mm for the HS and the lateral margin of the carotid canal and 34.5±2.0 mm for the HS and the medial margin of the carotid canal without distinction was made between the right and left sides. The linear distance between HS and the anterior tip of the foramen lacerum was 4.70±0.65 cm for the right and 4.77±0.70 cm for the left side. The linear distance between HS and the posterior tip of the foramen lacerum was 4.23±0.71 cm for the right and 4.25±0.55 cm for the left side. Ulug et al. described these values as anteromedial margin of the foramen lacerum and reported as 47.0±2.1 mm. The distance between HS and the posterolateral margin was also reported as 52.6±2.3 mm. For the jugular foramen, the only reported distance between the HS and posterolateral margin of the jugular foramen was 23.4±2.3 mm. In our study, the HS and lateral margin of the foramen lacerum were 1.68±0.29 cm and 1.78±0.39 cm for the right and left sides, respectively. When compared with this study, it is seen that our data have lower values. We think that this may be due to the difference in method since the measurement results of Ulug et al. were made with a caliper (3). We can say that, as far as we know, the angular measurements measured within the study are new in the literature, and therefore there is no data to compare. The age of the skulls, the year, and the region they belong to are not known. For this reason, differences in measurements may be expected results. There are studies showing that climate and geography have an effect on skull measurements (13).

The data in the literature are linear distance measurements and provide information about the topography of the region. In this study, in addition to the literature, we have shown the structure of the relevant region specific to the person through the correlation and relationships between anatomical structures with a different statistical approach.

A relational and functional understanding of skull base anatomy through appropriate mnemonic devices allows a neurosurgeon to maintain familiarity with regional anatomy despite potentially adverse conditions (3,14), such as distortion of native anatomy caused by a skull base tumor or subarachnoid hemorrhage (3). This distortion makes navigating complex regional anatomy intraoperatively more difficult, but relying on familiar landmarks can help the surgeon avoid potential complications. Being aware of the geometric relationships represented by the cranial triangles allows surgeons to quickly orient themselves according to the skull anatomy (3). The study shows a significant correlation between the common skull base cranial approaches and the parapetrosal triangle and some important anatomical structures within it that the surgeon should pay attention to during dissection. The importance of this area is that it can provide a guide to regional paraclival anatomy from an exocranial perspective. Using the regression formulas created using the relationship between the triangle and the anatomical formations within it, personalized and more reliable intervention areas were created. A different perspective was added to the field with the mathematical approach.

Limitations

The limitations of the study include the unknown age and gender of the bones used and the small number of bones. The study has shown that the parapetrosal triangle and the formations within it are correlated, and we recommend working with a larger number of bones of known size.

Conclusion

The parapetrosal triangle and the structures forming its border are important reference points in cranial surgeries. As a result of the high-reliability models that we created by taking the parapetrosal triangle as a reference, we showed that Henle's spine is a reliable reference point by the literature with a different method. Being able to predict the relationship between important anatomical structures in the interventions to be performed in the region can be a good guide for surgeons.

Disclosures

Acknowledgment: We thank to all the individuals who have donated their bodies as cadaver because of belief in science.

Peer-review: Externally peer-reviewed.

Author Contributions: Concept – N.T.Ç.; Design – N.T.Ç., S.D.Y.; Supervision – S.D.Y., S.B.; Materials – N.T.Ç., S.D.Y.; Data collection &/or processing – S.D.Y., S.B.; Analysis and/or interpretation – S.D.Y.; Literature search – N.T.Ç.; Writing – N.T.Ç.; Critical review – N.T.Ç, S.B.

Conflict of Interest: There is no any conflict of interest.

Funding: There is no any funding.

References

1. Cavallo LM, Messina A, Cappabianca P, Esposito F, de Divitiis E, Gardner P, Tschabitscher M. Endoscopic endonasal surgery of the midline skull base: anatomical study and clinical considerations. Neurosurg Focus. 2005;19(1):1-14. https://doi.org/10.3171/foc.2005.19.1.3
2. Gurumurthy K, Premavath D. Morphometric Analysis of Parapetrosal Triangle, International Journal of Pharmaceutical Research, 2020;Suppl(1):3536-39.
3. Ulug T, Ozturk A, Sahinoglu K. A multipurpose landmark for skull-base surgery: Henle's spine. J Laryngol Otol. 2005;119(11):856-61. https://doi.org/10.1258/002221505774783494
4. Parkinson D. A surgical approach to the cavernous portion of the carotid artery. Anatomical studies and case report. J Neurosurg. 1965, 23:474-483. https://doi.org/10.3171/jns.1965.23.5.0474
5. Parkinson D. Transcavernous repair of carotid cavernous fistula. J Neurosurg. 1967, 26:420 424. https://doi.org/10.3171/jns.1967.26.4.0420
6. Drazin D, Wang JM, Alonso F, Patel DM, Granger A, Shoja MM, Loukas M, Oskouian RJ, Tubbs RS. Intracranial Anatomical Triangles: A Comprehensive Illustrated Review. Cureus. 2017;4;9(10):e1741. https://doi.org/10.7759/cureus.1741
7. Hendricks BK, Benet A, Lawrence PM, Benner D, Preul MC, Lawton MT. Anatomical Triangles for Use in Skull Base Surgery: A Comprehensive Review. World Neurosurg. 2022;164:79-92. https://doi.org/10.1016/j.wneu.2022.04.038
8. Vijaywargiya M, Deopujari R, Athavale SA. Anatomical study of petrous and cavernous parts of internal carotid artery. Anat Cell Biol. 2017;50(3):163-170. https://doi.org/10.5115/acb.2017.50.3.163

9. Ray B, Rajagopal KV, Rajesh T, Gayathri BM, D'Souza AS, Swarnashri JV, et al. Morphometry and CT measurements of useful bony landmarks of skull base. Rom J Morphol Embryo 2011; 52(3): 873-877.
10. Senthil Kumar B, Vijaya Kumar J. Henle's Spine - an Anatomical Landmark for Approaching Various Foramina in the Base of Skull. Journal of Krishna Institute of Medical Sciences University. 2018;7(1):8-15.
11. Piromchai P, Wijewickrema S, Smeds H, Kennedy G, O'Leary S. Correlations of External Landmarks With Internal Structures of the Temporal Bone. Otol Neurotol. 2015;36(8):1366-73. https://doi.org/10.1097/MAO.0000000000000824
12. Maheshwari P, Parveen S, Kawatra R, Ashraf S, Perwin N. A Case Series of Positional Variations in the Spine of Henle: A Surgical Conundrum. Indian J Otolaryngol Head Neck Surg. 2023;75(4):4190-4193. https://doi.org/10.1007/s12070-023-04017-4
13. Canbay Durmaz S, BolatliG. Changes in human skull anatomy from past to today: Systematic review. Atlantic J Med Sci Res. 2024;4(4):102-8. https://doi.org/10.5455/atjmed.2024.09.016
14. Tangsrivimol JA, Abouammo MD, Prevedello DM. Endoscopic Anatomy of the Skull Base. Adv Tech Stand Neurosurg. 2024;52:29-61. https://doi.org/10.1007/978-3-031-61925-0_4